International Journal of Heat and Technology
Vol. 36, No. 4, December, 2018, pp. 1268-1275
Journal homepage:http://iieta.org/Journals/IJHT

Determination of a Hopf bifurcation of natural convection in a symmetric heated square cavity

Djoubeir Debbah[1], Omar Kholai[2], Abdelkader Filali[3]*

[1] Département de Génie Mécanique, Université des Frères Mentouri, Constantine 1, 25000, Algérie
[2] Laboratoire d'Ingénierie des Transports et Environnement, Département de Génie des Transports, Université des Frères Mentouri, Constantine 1, 25000, Algérie
[3] Department of Chemical Engineering, Imperial College London, London SW7 2AZ, United Kingdom

Corresponding Author Email: f.abdelkader@imperial.ac.uk

https://doi.org/10.18280/ijht.360415

Received: 31 May 2018
Accepted: 15 December 2018

Keywords:
critical rayleigh number, finite volume method, fft, natural convection, Hopf bifurcation, transient regime

ABSTRACT

In the present study, numerical investigation is carried out to analyze natural convection in symmetrically heated square cavity filled with air. Left, right and bottom walls are heated partially, whereas remaining portions of these walls are maintained at a lower constant temperature with an isolated top wall. Governing equations are solved by a finite volume method and the analysis is conducted for different Rayleigh number Ra values ranged between 10^3 and $9x10^6$. The objective of the present study is to determine the critical Rayleigh number in which a transition from a stationary to an oscillatory flow takes place. The effect of the heating sources placed symmetrically at the two opposite sidewalls in addition to the heating source at the bottom wall was investigated. Results are presented in terms of streamlines, isotherms, and flow variables including the velocity and, temperature profiles and, Fourier frequency spectrum of the temperature. Obtained results shown that for Rayleigh numbers smaller than $Ra_{cr} = 3 \times 10^6$, the flow inside the cavity remains stationary with perfectly symmetric patterns. Whereas, beyond this critical value, the system bifurcates in which the flow symmetry is broken and a first Hopf time dependent periodic flow patterns take place.

1. INTRODUCTION

Natural convection in a square and/or rectangular cavity with partially heated wall problem is of great interest and frequently encountered in different engineering applications, including solar energy, nuclear reactor design, cooling of electrical and electronic components and heat exchange between buildings and environment.

In the past few decades, several investigations have been carried out on the analysis of the flow and heat transfer for natural convection problem in a four-sided cavity with fully or partially heated walls. Rahman et al. [1] investigated the natural convection problem in four-sided cavity with the presence of heat generation using numerical technique. A partially heater was positioned at several locations on the right wall of the cavity, whereas the left wall was kept at lower temperature. Results showed that the flow and heat transfer rate are strongly dependent on the length and locations of the heater as well as heat generating parameter. Other researchers such as Corcione [2], Basak [3], El Moutaouakil et al. [4] and Aswatha et al. [5], have investigated the natural convection problem in a square cavity under different applied thermal boundary conditions.

Various published papers that included the study of transient natural convection in rectangular or square enclosures in which different experimental and numerical approaches were adopted and described in detail [6]. An important fact for natural convection flows in rectangular enclosures is that the thermal boundary layer adjacent to the vertical walls remains steady and provides perfectly symmetric flow at small Rayleigh numbers. However, at sufficiently large Rayleigh numbers, the thermal boundary layer distinct travelling waves owing to convective instability [7].

Saury et al. [8] study experimentally the instability phenomena which appear in natural convection in air-filled cavities with active isothermal walls heated differentially, the other walls being adiabatic. The cavity is inclined by an angle varying between 0° (heating from the bottom) and 180° (heating from the top). Instantaneous measures enable localizing regions presenting maximal temperature fluctuations when the temperature difference between the active walls increases. In order to determine the routes to chaos, Kieno et al. [9] investigated numerically the natural convection problem in an enclosure inclined to the horizontal plane. This enclosure is heated from two opposite side and cooled on the other two sides. The impact of Rayleigh number and the inclination angle are examined in detail. The analysis confirms also the bifurcation of the attractor from a limit point to a limit cycle via an overcritical Hopf bifurcation for a Rayleigh number between $1.95x10^6$ and $1.96x10^6$. Sheu and Lin [10] carried out numerical investigation for natural convection problem in cubic cavity over a wide range of Rayleigh numbers by the simulated bifurcation diagram, limit cycle, power spectrum and phase portrait. Results indicated that for successive increase in Rayleigh number, the predicted flow is found to change from the steady and symmetric laminar solution to the asymmetric state (pitchfork bifurcation) and then to supercritical Hopf bifurcation. As the Rayleigh number is increased still, the investigated buoyancy-driven

flow became increasingly destabilized through quasi-periodic bifurcation and then through two predicted frequency-doubling bifurcations. Then an additional ultra-harmonic frequency showed its presence prior to chaos.

Benouaguef et al. [11] carried out numerically the time dependent natural convection in a square cavity heated partially on the two opposite vertical walls. The two opposite heaters were maintained at different temperatures whereas the horizontal walls were considered adiabatic. A first transition from stable steady solution to oscillatory flow could be characterized at Ra ranging from $2.5x10^5$ to $2.51x10^5$ and the second subharmonic bifurcation that evolves into a chaotic flow could be obtained as Rayleigh number was increased further ($Ra > 2.51x10^5$). Later, Xu, and Saha [12] and Kolsiet et al. [13] investigated numerically the transition from steady-state to a transient flow in air-filled cavity. Different values of Rayleigh number ranging from 10^5 to 10^9 were investigated and results showed that the transition from a steady-state to a periodic flow arises as Rayleigh number increases. The numerical study presented by Laouar et al. [14] was to follow the bifurcation sequences to chaos and to investigate different flow regimes including, periodic, quasi-periodic and the chaotic regimes.

Zhao and Tian [15] proposed higher-order accuracy method for the solution of time-dependent nature convection problem in square enclosure with adiabatic horizontal walls and differentially heated vertical walls for the wide range of Rayleigh numbers ($10^3 < Ra < 10^{10}$). An optimized third-order upwind compact scheme (Opt-UCD3) and a fourth-order symmetrical Padé compact scheme used to approximate the nonlinear convective terms and the viscous terms, respectively. Results showed that a first Hopf bifurcation to the periodic flow regime could be obtained at $Ra_{c1} = 1.82 \times 10^8$, and then undergoes second bifurcation to quasi-periodic flow regime could be obtained at a critical Rayleigh number $2.25 \times 10^8 < Rac2 < 2.35 \times 10^8$ and eventually transits to turbulent through a further bifurcation.

The main objective of the present study is to determine the critical Rayleigh number which is the bifurcation point of stationary flow to oscillatory flow, when increasing the Rayleigh number in a square enclosure that was locally discrete heated (the length of this heat source is L/2) from below and two others heating portions (with the length of L/4) mounted symmetrically on the two vertical side walls. These suggested locations may occur in different engineering applications such as improvement of cooling process for electronic equipment. This study is carried out numerically using a developed code based on finite volume method and SIMPLE algorithm was used for the coupling of the velocity and pressure variables. Simulations are conducted for a range of Rayleigh number Ra between 10^3 and $9x10^6$. The influence of Ra number on the flow patterns, the local temperature variation, and the heat transfer rate in the square cavity are analyzed and discussed.

2. MATHEMATICAL MODEL

The geometrical model investigated in the present study is a square cavity with a sidewall length L as shown in Figure 1. A heater source of a length (L/2) is placed at the center of the bottom wall and maintained at a higher temperature T_h, whereas two other heater sources with same temperature are placed at the two opposite vertical sidewalls with a length equal to (L/4) and mounted at L/4 from the bottom wall. Remaining parts of the bottom, left and right sidewalls are maintained at a lower temperature T_C and the top is insulated. The flow regime is considered laminar, incompressible and fluid properties are supposed constant excluding the density in which buoyancy forces are not neglected and follow the Boussinesq approximation. In general, when natural convection mechanism is considered, radiation may have considerable effects. However, in some case, these effects can be neglected (low temperatures involved and or boundaries with very low emissivity or when the used fluid is assumed to be perfectly transparent to radiation) [16-18]. In the present study, since we are interested in flows induced by small temperature levels, radiation and viscous dissipation effects are ignored. The length of the third dimension of the cavity perpendicular to the plane of the sketch is supposed to be sufficiently long, thus the flow can be considered two-dimensional. Governing equations for transient natural convection flow can be summarized as follows:

$$\frac{\partial u}{\partial x}+\frac{\partial v}{\partial y}=0 \tag{1}$$

$$\frac{\partial u}{\partial t}+u\frac{\partial u}{\partial x}+v\frac{\partial u}{\partial y}=-\frac{1}{\rho}\frac{\partial p}{\partial x}+\nu\left(\frac{\partial^2 u}{\partial x^2}+\frac{\partial^2 u}{\partial y^2}\right) \tag{2}$$

$$\frac{\partial v}{\partial t}+u\frac{\partial v}{\partial x}+v\frac{\partial v}{\partial y}=-\frac{1}{\rho}\frac{\partial p}{\partial y}+\nu\left(\frac{\partial^2 v}{\partial x^2}+\frac{\partial^2 v}{\partial y^2}\right)+g\beta(T-T_C) \tag{3}$$

$$\frac{\partial T}{\partial t}+u\frac{\partial T}{\partial x}+v\frac{\partial T}{\partial y}=\alpha\left(\frac{\partial^2 T}{\partial x^2}+\frac{\partial^2 T}{\partial y^2}\right) \tag{4}$$

with the applied boundary conditions at the four cavity walls:

$$u(x,0)=u(x,L)=u(0,y)=u(L,y)=0;$$
$$v(x,0)=v(x,L)=v(0,y)=v(L,y)=0;$$

On the heated part:

$$T(x,0)=T(0,Y)=T(L,y)=T_h;$$

On the cooled part:

$$T(x,0)=T(0,Y)=T(L,y)=T_C;$$

On the top wall:

$$\frac{\partial T}{\partial y}=0 \tag{5}$$

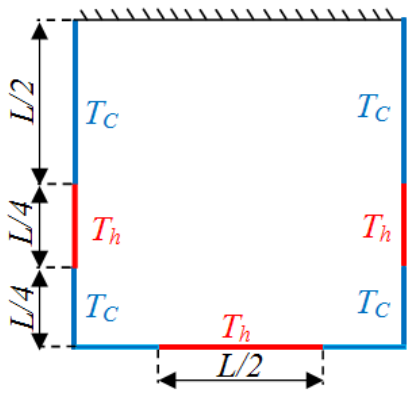

Figure 1. Schematic of enclosure configuration

Introducing the following dimensionless variables:

$$X=\frac{x}{L}\ ,\ Y=\frac{y}{L}\ ,\ U=\frac{uL}{\alpha}\ ,\ V=\frac{vL}{\alpha}\ ,\ P=\frac{pL^2}{\rho\alpha^2}\ ,\ \theta=\frac{(T-T_C)}{(T_h-T_C)}\ ,$$
$$\tau=\frac{\alpha t}{L^2}\ ,\ Pr=\frac{\upsilon}{\alpha}\ ,\ Ra=\frac{g\beta(T_h-T_C)L^3\,Pr}{\upsilon^2} \qquad (6)$$

Substituting the dimensionless variables into the dimensional equations, we obtain the non-dimensional system equations:

$$\frac{\partial U}{\partial X}+\frac{\partial V}{\partial Y}=0 \qquad (7)$$

$$\frac{\partial U}{\partial \tau}+U\frac{\partial U}{\partial X}+V\frac{\partial U}{\partial Y}=-\frac{\partial P}{\partial X}+Pr\left(\frac{\partial^2 U}{\partial X^2}+\frac{\partial^2 U}{\partial Y^2}\right) \qquad (8)$$

$$\frac{\partial V}{\partial \tau}+U\frac{\partial V}{\partial X}+V\frac{\partial V}{\partial Y}=-\frac{\partial P}{\partial Y}+Pr\left(\frac{\partial^2 V}{\partial X^2}+\frac{\partial^2 V}{\partial Y^2}\right)+Pr\,Ra\,\theta \qquad (9)$$

$$\frac{\partial \theta}{\partial \tau}+U\frac{\partial \theta}{\partial X}+V\frac{\partial \theta}{\partial Y}=\left(\frac{\partial^2 \theta}{\partial X^2}+\frac{\partial^2 \theta}{\partial Y^2}\right) \qquad (10)$$

with the applied boundary conditions at the four cavity walls:

$$U(X,0)=U(X,L)=U(0,Y)=U(L,Y)=0;$$
$$V(X,0)=V(X,L)=V(0,Y)=V(L,Y)=0;$$

On the heated part:

$$\theta(X,0)=\theta(0,Y)=\theta(L,Y)=1;$$

On the cooled part:

$$\theta(X,0)=\theta(0,Y)=\theta(L,Y)=0;$$

On the top wall:

$$\frac{\partial \theta}{\partial Y}=0 \qquad (11)$$

Along the heated part of the side walls, the calculated local heat transfer rate is obtained from the heat balance that provides a formulation of the local Nusselt number as follows:

$$Nu_h(X)=\left.\frac{\partial\theta}{\partial Y}\right|_{Y=0}\ ,\ \frac{L}{4}\le X\le\frac{3L}{4}$$
$$Nu_h(Y)=\left.\frac{\partial\theta}{\partial X}\right|_{X=0,X=L}\ ,\ \text{(along the heated section)} \qquad (12)$$

The average Nusselt number Nu_h on heaters is calculated by:

$$\overline{Nu_h}(X)=\frac{1}{L/2}\int_{L/4}^{3L/4}\left.\frac{\partial\theta}{\partial Y}\right|_{Y=0}dX$$
$$\overline{Nu_h}(Y)=\frac{1}{L/4}\int_{Y_1}^{Y_2}\left.-\frac{\partial\theta}{\partial X}\right|_{X=0,X=L}dY\ ,\ \text{(along the heated section)} \qquad (13)$$

3. SOLUTION PROCEDURE

Governing equations for the simulation of natural convection problem in a square cavity are numerically solved according to the applied boundary conditions. These governing equations were discretized using the finite volume method yielding a system of algebraic equations, Patankar [19]. After several attempts of the different numerical schemes, we have opted to the central differencing scheme to approximate the combined convection and diffusion terms. This scheme always gives a physically valid solution of the unsteady problems with respect to higher order schemes. The continuity equation is transformed into a pressure correction equation according to the SIMPLE algorithm to overcome the velocity and pressure field coupling problem. In the X and Y sweeping direction, the resulting linear algebraic system is solved using the Tri-Diagonal Matrix Algorithm (TDMA). The unconditionally stable implicit method is used to evaluate the transient terms in momentum and energy equations. In the present study, a (100 x 100) uniform mesh was used for all computations and a time step of $\Delta t = 2.5\text{x}10^{-5}$s.

4. GRID INDEPENDENCE TESTANDCODE VALIDATION

Grid sensitivity tests were performed first to calculate the local variation of the velocity and temperature profiles for Ra = 10^3 and, for different meshes of 40x40, 80x80, 100x100 and 110x110.

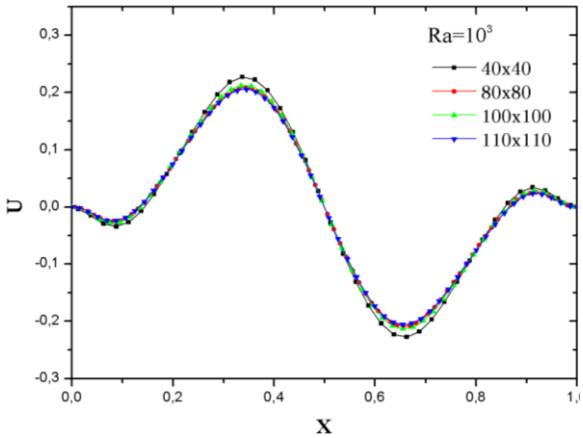

(a)

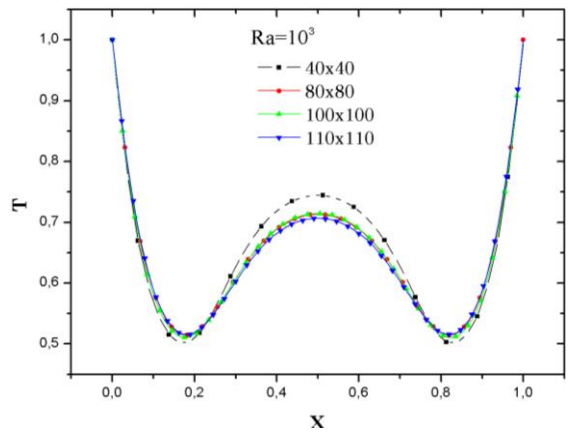

(b)

Figure 2. Grid independence study for Ra=10^3: (a) horizontal velocity profile and (b) temperature profile, at the mid-height of the cavity

Figures 2a and 2b shows the variation of the velocity component in x direction and the temperature throughout the

horizontal midline enclosure for the different meshes considered. It can be noticed that the changes in the calculated values are very small for three meshes of 100x100 and, 110x110 meshes is less than 0.00911= 0.911%. Hence, the mesh of 100x100 was chosen in the present study which providesthe best compromise between cost and accuracy of calculations.

The performance and the accuracy of the present numerical approach is investigated in a second step by comparing the present results with the numerical solution obtained by De Vahl [20]. Comparison of the maximum stream function for two different Rayleigh numbers is presented in Table 1. A maximum difference of about 0.18% is obtained which indicates a good agreement of the present results with the data presented by De Vahl [20].

Table 1. Comparison of of the maximum stream functionwith the results obtained by De Vahl [20]

Ra	De Vahl Davis	Present study
	$\|\psi\|_{max}$	$\|\psi\|_{max}$
10^5	9.612	9.5898
10^6	16.750	16.719

A second validation is conducted by comparing the present numerical results with the experimental data provided by Calcagni et al. [6]. The case investigated is an experimental investigation of free convective heat transfer in a square cavity in which a discrete heater is placed at the bottom wall whereas the lateral walls are cooled.

As shown in Figure 3, present numerical results for the variation of the local Nusselt (Nu) are compared with the data of Calcagni et al. [6] for Rayleigh number equal to $6.1x10^4$. Results indicate a good agreement between the present results and the measured data.

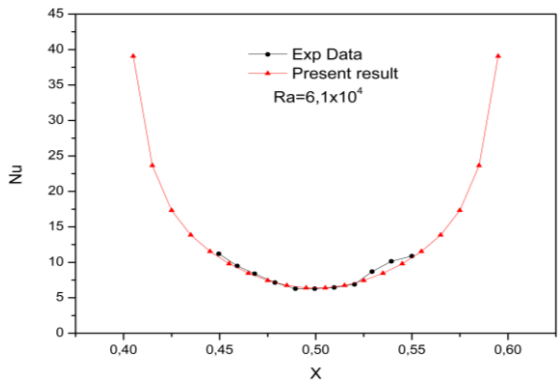

Figure 3. Comparison of the calculated local Nusselt on the heat source (x-axis) with experimental data [6]

5. RESULTS AND DISCUSSION

Present numerical simulation is performed for air fluid with Pr = 0.71. Results in the form of velocity and temperature profiles, streamline and isothermal contours for two cases including symmetric (stable) and asymmetric (oscillating) flow regimes will be presented and discussed.

Case 1: Stable flow regime at $Ra=3.1x10^3$

Figure 4 show the isotherms and streamlines inside the cavity, for low values of Ra number. The flow patterns are perfectly symmetric about the vertical axis consisting of two primary convective vortices and two weak vortices on the low corners of the cavity rotating in the opposite direction. In this regime, the intensity of both vortices on the left and right sides is identical, and the flow and heat transfer are influenced and controlled by the heater on the bottom wall whereas the effect of the two opposite heaters is minor and has no sufficient influence on the flow field.

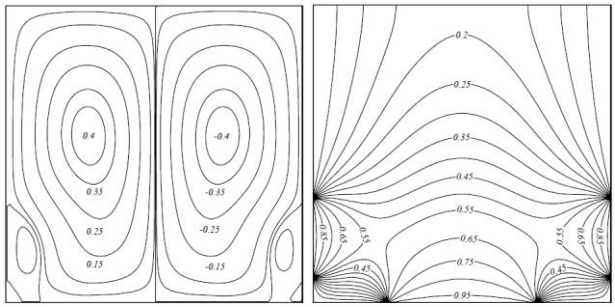

Figure 4. Isotherms (right) and streamlines (left) contours for $Ra=3,1x10^3$

Case 2: Oscillating flow regime at $Ra_{Cr} = 3x10^6$

As Rayleigh number increases, the size and number of the secondary vortices increases at the advantage of the primary vortices and, the flow symmetry is broken. As shown in Figure 5, between Rayleigh number values of $3,1x10^3$ and $3x10^6$, the flow bifurcates from a stable symmetric to instable asymmetric state. Hence, the onset of this bifurcation counted for the Rayleigh critical number of $3x10^6$. At this critical value $Ra_{Cr} = 3x10^6$, instabilities arise due to the force competition between the main and the secondary vortices, causing the flow to lose symmetry and an oscillatory flow field prevails. It should be noted that in this solution, the temperature contours oscillate with a small frequency in the right sidewalls. In this instable flow regime, the two previously symmetric vortices (shown in figure 4) became asymmetric with different sizes and different intensities (as shown in figure 5) in which the stream function values are -40 and 70 for the small vortex at the top of he cavity and the larger vortex at the bottom of the cavity, respectively, confirming the unbalance flow strength in the two regions. In this regime, the effect of the two opposite heaters is important and has a significant influence on the flow field and heat transfer levels.

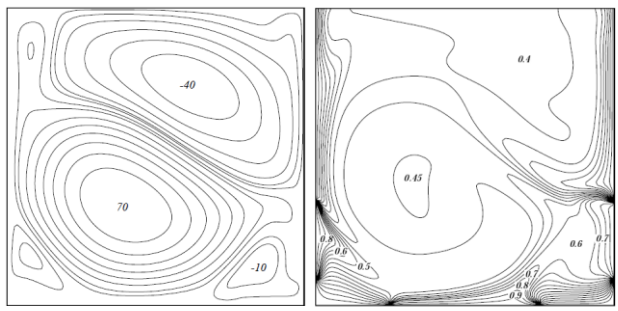

Figure 5. Isotherms (right) and Streamlines (left) contours for $Ra_{Cr}=3x10^6$

The temporal progress of the temperature, and velocity components calculated in the center of the enclosure, for two

Rayleigh numbers are presented in Figures 6 and 7, respectively. It can be noticed that for Ra = $3{,}1x10^3$ a steady-state solution could be obtained, whereas for $Ra_{Cr} = 3x10^6$ the solution oscillates with a mono-period of oscillation.

The temporal spectrum of the temperature at the point (x = 0.5, y = 0.5) at $Ra_{Cr} = 3x10^6$ is shown in Figure 8 (a) and is characterized by a main frequency (with harmonics) of f1 = 0.012.

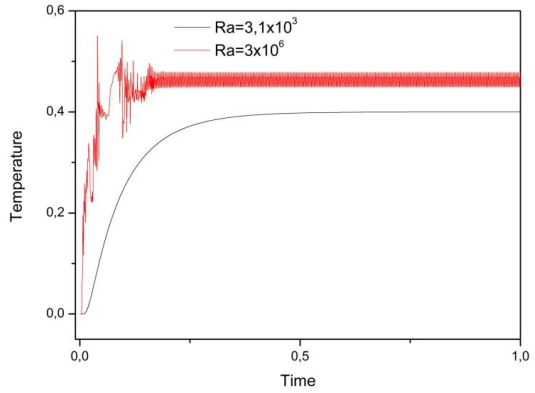

Figure 6. Time-distributions of Temperature at the mid-point for Ra=$3{,}1x10^3$ and $Ra_{Cr}=3x10^6$

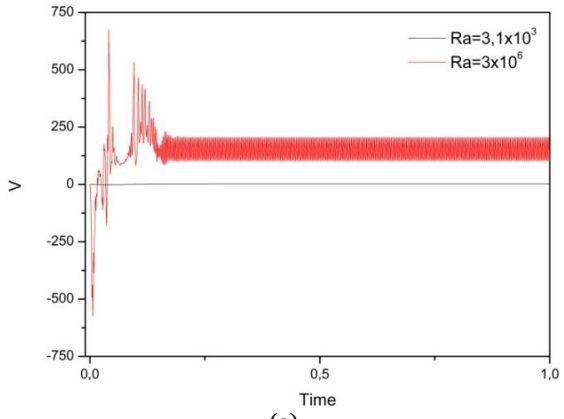

(a)

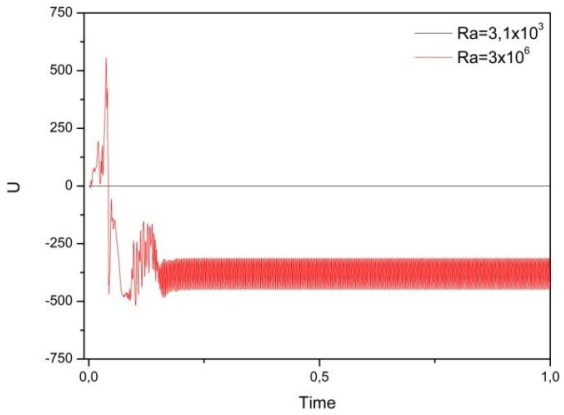

(b)

Figure 7. Time-distributions of V (a) and U (b) at the mid-point for Ra=$3{,}1x10^3$ and $Ra_{Cr}=3x10^6$

For Rayleigh number smaller than $Ra_{Cr} = 3 \times 10^6$, the system is at fully stationary state. Beyond this critical value, the system bifurcates and indicates a periodic movement of the flow; see Figure 8 (b).

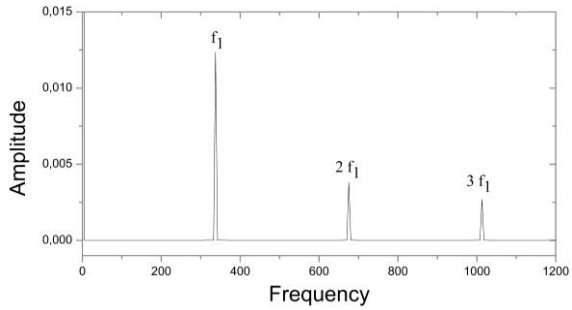

(a)

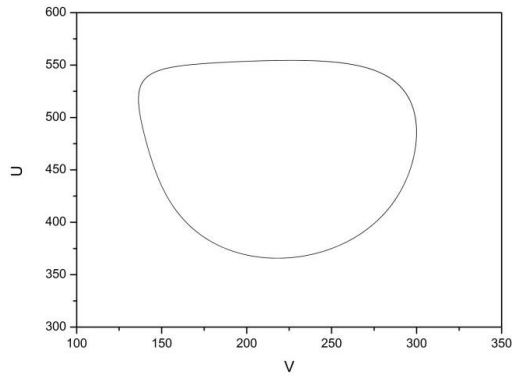

(b)

Figure 8. Fourier spectra (a) of T and V and U (b) at the mid-point for Ra=$3x10^6$

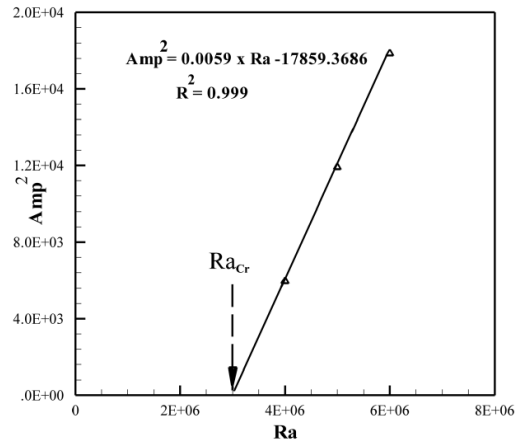

Figure 9. Variation of the square amplitude of U-velocity at the point (0.5,0.5) as function of Ra number

It should be noted that the appearance of oscillatory instability is linked to the fact that the flow loses its stability through a Hopf bifurcation [21]. To make sure that this is a Hopf bifurcation type, we proceed as follows: for a supercritical Hopf bifurcation, the amplitude of the periodic solutions is proportional to $(Ra - Ra_{Cr})^{1/2}$, so first we have calculated the supercritical solutions for different values of Ra in the vicinity of Ra_{Cr} in order to avoid any amplitude modulation effect, then, we have examined the relation between the amplitude A_{amp} of the solutions and the number of Ra. Finally, we could extrapolate the results to $A_{amp} = 0$ to obtain Ra_{Cr}. Figure 9 present the curve $\left(A_{amp}^2 - Ra\right)$, in which quasi-linear relation could be obtained (the coefficient of determination of the fitting curve is $R^2 = 0.999$ which represents high linear fitting degree with the obtained data), thus, confirms that the bifurcation is supercritical. The

extrapolation of this curve provides the Critical Rayleigh number which equal to $Ra_{Cr} = 3x10^6$.

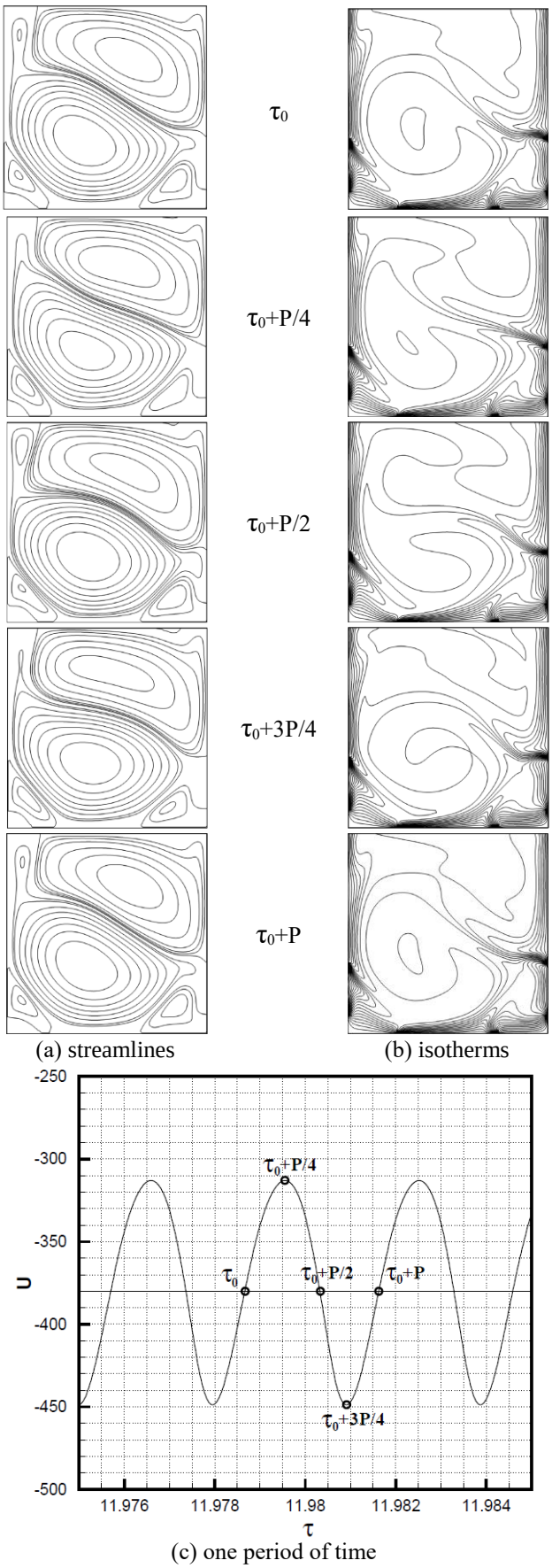

Figure 10. Temporal evolution of (a) the streamlines and (b) the isotherms during (c) one oscillation period for Ra_{Cr}

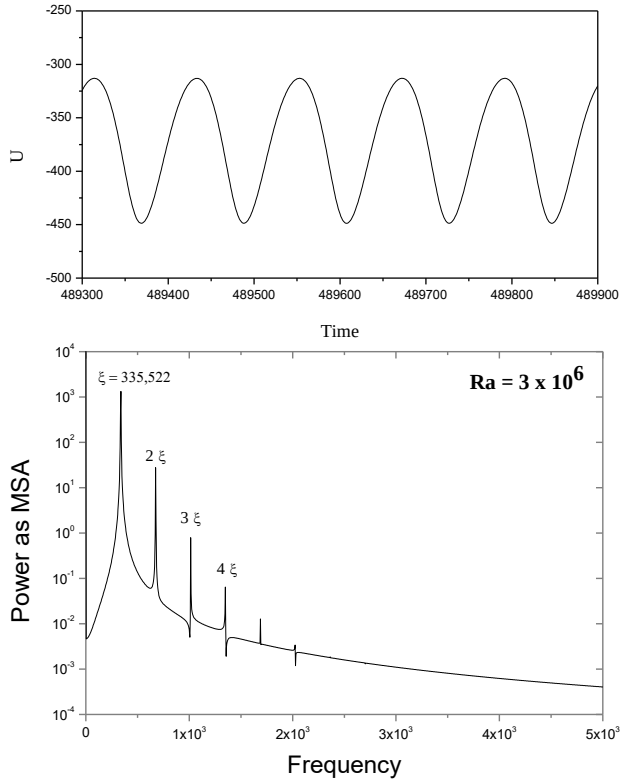

Figure 11. Temporal evolution of U-velocity for Ra_{Cr} and the corresponding energy spectra

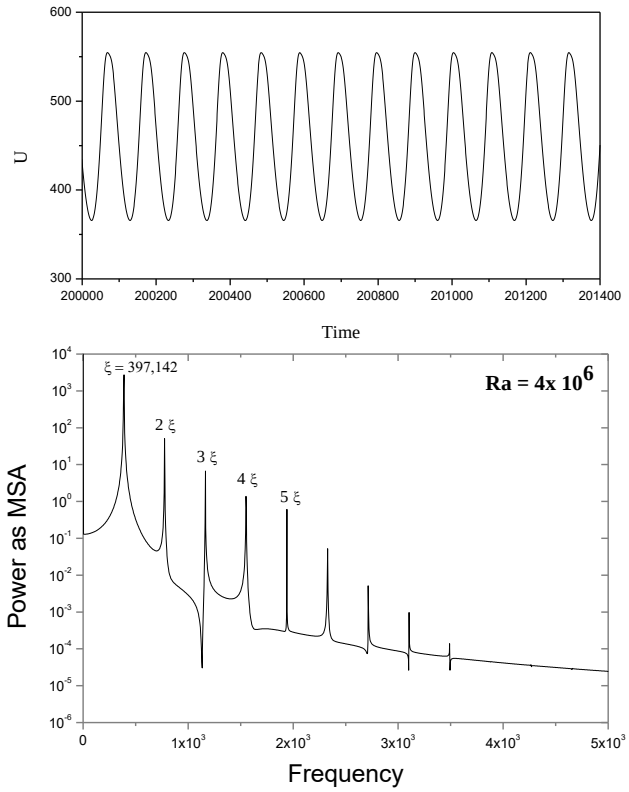

Figure 12. Temporal evolution of U-velocity for Ra =4 $x10^6$and the corresponding energy spectra

To determine the fundamental frequency and these harmonics characteristics, Fourier transform is used. To better explain the phenomenon and give some information on the spatial structure, we have analyzed the oscillatory evolution of the flow field and temperatures versus time. Figure 10 shows

the streamlines and isotherms during one period. The oscillatory nature of the velocity U in the middle of the cavity for Ra = $3x10^6$, indicates that the periodicity of the instabilities is related to the dilatation, the narrowing of the main and secondary cells and to the birth of new secondary cells.

The power spectrum for Ra = 3×10^6 and 4×10^6 shown in Figures 11 and 12 has been calculated from the temporal evolution of the horizontal velocity U in the middle of the cavity. This spectrum illustrates the presence of a base frequency ξ = 335.522 and ξ = 397.142 and their odd harmonics. As the critical Rayleigh number increases, the amplitudes of the oscillations become larger, while their periods δ become shorter, see Figure13 (an increase in the fundamental frequency).

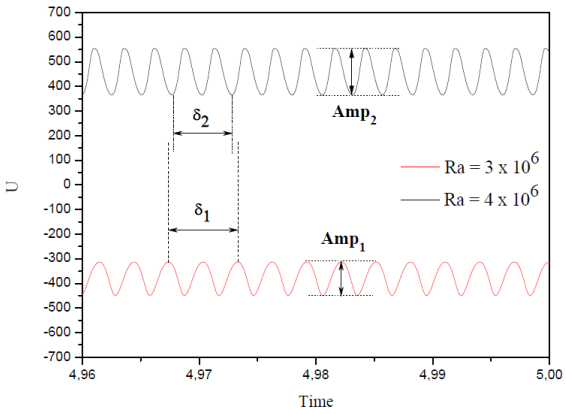

Figure 13. Temporal evolution of U-velocity for Ra =3 $x10^6$ and Ra = 4 $x10^6$

6. CONCLUSIONS

In this study, stability of natural convection in symmetrically heated square cavity filled with air is investigated. The critical Rayleigh number in which a transition from a stationary to an oscillatory flow takes place is determined.

The flow pattern at Ra=$3.1x10^3$ is perfectly symmetric consisting of two primary convective vortices and two weak vortices near the heated portions of the sidewall, which rotate in opposite directions. The intensity of both eddies in this flow regime is identical due to the symmetry in boundary conditions applied at the vertical walls, and the value of the stream function along the symmetry line is zero.

For Ra_{Cr}= $3x10^6$, the flow bifurcates from a stable symmetric to stable asymmetric state. Hence, the onset of this bifurcation counted for the Rayleigh critical number of $3x10^6$. At this critical value Ra_{Cr} =$3x10^6$, instabilities arise due to the force competition between the main and the secondary vortices, causing the flow to lose symmetry and an oscillatory flow field prevails. The solution at this value of Rayleigh number is mono-periodic with one frequency f1=0.012, and the curve of V versus U is closed.

As the critical Rayleigh number increases, the amplitudes of the oscillations become larger, while their periods δ become shorter (an increase in the fundamental frequency).

REFERENCES

[1] Rahman MM, Mamun MAH, Billah MM, Saidur R. (2010). Natural convection flow in a square cavity with internal heat generation and a flush mounted heater on a side wall. Journal of Naval Architecture and Marine Engineering 7: 37-50. http://dx.doi.org/10.3329/jname.v7i2.3292

[2] Corcione M. (2003). Effects of the thermal boundary conditions at the sidewalls upon natural convection in rectangular enclosures heated from below and cooled from above. International Journal of Thermal Sciences 42: 199–208. https://doi.org/10.1016/S1290-0729(02)00019-4

[3] Basak T, Roy S, Balakrishnan AR. (2006). Effects of thermal boundary conditions on natural convection flows within a square cavity. International Journal of Heat and Mass Transfer 49: 4525-4535. https://doi.org/10.1016/j.ijheatmasstransfer.2006.05.015

[4] El Moutaouakil L, Zrikem Z, Abdelbaki A. (2013). Convection naturelle multicellulaire dans une cavité verticale allongée: Effets des conditions aux limites non uniformes. 16èmes Journées Internationales de Thermique (JITH 2013) Marrakech (Maroc).

[5] Aswatha CJ, Gangadhara Gowda SN, Sridhara KN. (2013). Effect of convective boundary conditions at bottom wall on natural convection in a square cavity. Journal of Engineering Science and Technology 8(2): 141-164.

[6] Calcagni B, Marsili F, Paroncini M. (2005). Natural convective heat transfer in square enclosures heated from below. Applied Thermal Engineering 25: 2522–253. https://doi.org/10.1016/j.applthermaleng.2004.11.032

[7] Xu F, Patterson JC, Lei C. (2014). An experimental study of the coupled thermal boundary layers adjacent to a partition in a differentially heated cavity. Exp. Therm Fluid Sci. 54: 12-21. https://doi.org/10.1016/j.expthermflusci.2014.01.005

[8] Saury D, Benkhelifa A, Penot F. (2012). Experimental determination of first bifurcations to unsteady natural convection in a differentially heated cavity titled from 0° to 180°. Experimental Thermal and Fluid Science 38: 74-84. https://doi.org/10.1016/j.expthermflusci.2011.11.009

[9] Kieno PF, Ouédraogo A, Zongo OM, Bathiébo JD, Zeghmati B. (2013). Numerical study of the routes toward chaos of natural convection within an inclined enclosure. J. Sci. Res. 5: 105-117. https://doi.org/10.3329/jsr.v5i1.10709

[10] Sheu T, Lin RK. (2011). Three-dimensional bifurcations in a cubic cavity due to buoyancy-driven natural convection. International Journal of Heat and Mass Transfer 54: 447-467. https://doi.org/10.1016/j.ijheatmasstransfer.2010.09.024

[11] Benouaguef SA, Zeghmati B, Bouhadef K, Daguenet M. (2008). Multiple solutions in natural convection in an air filled square enclosure: Fractal dimension of attractors. Journal of Applied Sciences 8(2): 218-229. https://doi.org/10.3923/jas.2008.218.229

[12] Xu F, Saha SC. (2014). Transition to an unsteady flow induced by a fin on the sidewall of a differentially heated air-filled square cavity and heat transfer. International Journal of Heat and Mass Transfer 71: 236-244. https://doi.org/10.1016/j.ijheatmasstransfer.2013.12.019

[13] Kolsi L, Hamida B, Hassen MB, Hussein W, Borjini AK, Sivasankaran MN, Saha S, Awad SC, Fathinia MMF, Ben Aissia H. (2015). Experimental and numerical

investigations of transient natural convectionin differentially heated air-filled tall cavity. American Journal of Modern Energy 1(2): 30-43. https://doi.org/10.11648/j.ajme.20150102.12

[14] Laouar S, Mezaache E, Daguenet M. (2005). Bifurcation to chaos in a non-uniformly heated vertical square cavity. International Meeting on Heat Transfer, Tanger, Morocco 1: 263-266.

[15] Zhao B, Tian Z. (2016). High-resolution high-order upwind compact scheme-based numerical computation of natural convection flows in a square cavity. International Journal of Heat and Mass Transfer 98: 313-328. http://dx.doi.org/10.1016/j.ijheatmasstransfer.2016.03.032

[16] El Ayachi R, Hasnaoui RA, Naïmi M, Abdelbaki A. (2012). Combined effects of radiation and natural convection in a square cavity submitted to two combined modes of cross gradients of temperature. Numerical Heat Transfer, Part A: Applications. 62: 905–931. https://doi.org/10.1080/ 10407782.2012.712463

[17] Benouaguef SA, Zeghmati B, Bouhadef K, Daguenet M. (2008). Multiple solutions in natural convection in an air filled square enclosure: Fractal dimension of attractors. Journal of Applied Sciences 8: 218-229. https://doi.org/10.3923/jas.2008.218.229

[18] Randriazanamparany MA, Skouta A, Daguenet M. (2005). Numerical study of the transition toward chaos of two-dimensional natural convection within a square cavity. Numerical Heat Transfer, Part A: Applications 48(2): 127-147. https://doi.org/10.1080/10407780490454386

[19] Patankar SV. (1980). Numerical Heat Transfer and Fluid Flow, McGraw-Hill, New York.

[20] De Vahl GD. (1983). Natural convection of air in a square cavity a bench mark numerical solution. International Journal for Numerical Methods in Fluids 3: 249-264. https://doi.org/10.1002/fld.1650030305

[21] Le Quéré P. (1990). Transition to unsteady natural convection in a tall water-filled cavity. Physics of Fluids. 2(4): 503-515. https://doi.org/10.1063/1.857750

NOMENCLATURE

g	gravitational acceleration, $m.s^{-2}$
L	width of the cavity, m
Nu	local Nusselt number along the heat source
P	pressure, Pa
Pr	Prandtl number
Ra	Rayleigh number
t	Dimentional time, s
u, v	Velocity component in x- and y- directions
U, V	Dimensionless velocity components
x, y	horizontal and vertical coordinates
X, Y	Dimensionless coordinates

Greek symbols

α	thermal diffusivity, $m^2. s^{-1}$
β	thermal expansion coefficient, K^{-1}
λ	thermal conductivity, $W. M^{-1}.K^{-1}$
ρ	density, $kg. m^3$
θ	dimensionless temperature, $(T-T_C)/(T_h-T_C)$
υ	fluid kinematic viscosity, $kg. m^{-1}.s^{-1}$
ψ	dimensional vorticity
τ	dimensionless time
δ	period
ξ	frequency

Subscripts

C	cold temperature
h	hot temperature
cr	critical number